Analysis of the Dynamic Responses of SOA Wavelength Converters Using Linear Frequency Resolved Gating Technique

A. Perez-Pardo, T. T. Ng, P. Petropoulos, S. Sales, *Senior Member, IEEE*, and D. J. Richardson

***Abstract*—This letter demonstrates the applicability of the linear frequency resolved optical gating technique for the complete characterization of the fast dynamic response of semiconductor optical amplifiers (SOAs) when operating as wavelength converters. We have investigated both the cross-gain modulation and cross-phase modulation responses to short pump signals, using an SOA Mach–Zehnder interferometer in a pump–probe configuration. A blind deconvolution algorithm has then been used to retrieve the electric field profiles of both the signal and the gate function.**

***Index Terms*—Dynamic response, optical data processing, phase measurement, semiconductor optical amplifiers (SOAs).**

I. Introduction

SEMICONDUCTOR optical amplifiers (SOAs) are of considerable interest as nonlinear optical processing devices, since they can facilitate such operations as signal regeneration and wavelength conversion. All-optical processing of signals in SOAs usually employs either cross-gain modulation (XGM) or cross-phase modulation (XPM). In the latter case, it is common to use integrated SOA Mach–Zehnder interferometers (SOA-MZIs) in order to convert phase changes into intensity variations. As the signal repetition rates approach the operating bandwidth of the SOA devices, precise knowledge of the response of the devices (in both intensity and phase) becomes ever more crucial.

Previous measurements of fast SOA phase responses have either involved measurements of the alpha characteristic [1] or used interferometric setups [2]. While the alpha characteristic is a useful indicator, it does not provide a detailed appreciation of the phase profile of the SOA response. Interferometric setups on the other hand, can be quite involved and are prone to environmental instabilities. Frequency resolved optical gating (FROG) on the other hand, has already been established in the laser community as a reliable technique for the characterization of short pulses both in amplitude and in phase. Several variations of FROG exist, of which linear FROG (L-FROG) is particularly attractive for the characterization of telecommunication signals, since it provides high sensitivity, is highly stable, and its implementation requires only off-the-shelf all-fiberized equipment [3]. L-FROG has already been employed for the characterization of laser pulses, transmission signals [4], and even for the measurement of the complex response of passive optical filters [5]. In this work, by measuring the response of an SOA-MZI to short pulses we demonstrate that L-FROG can readily be applied for the characterization of active devices. Using an SOA-MZI in a pump–probe configuration, we have investigated both the XGM and XPM response to short pump pulses. Through this study, we hope to provide a better understanding of the nonlinear behaviour of SOA devices which should aid the optimization of these versatile devices.

Manuscript received July 31, 2007; revised December 9, 2007. This work was supported in part by the Spanish Ministerio de Educación through the project TEC2007-68065-C03-01 and in part by the BONE-project, a Network of Excellence funded by the European Commission through the 7th ICT-Framework Programme.

A. Perez-Pardo and S. Sales are with the Optical and Quantum Communications Group, ITEAM Research Institute, Universidad Politécnica de Valencia, Camino de Vera s/n, 46022, Spain.

T. T. Ng, P. Petropoulos, and D. J. Richardson are with the Optoelectronics Research Centre, University of Southampton, Southampton SO17 1BJ, U.K.

Digital Object Identifier 10.1109/LPT.2008.924294

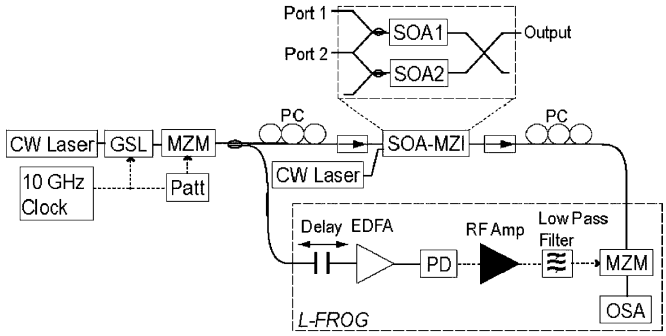

Fig. 1. Experimental setup of the SOA-MZI characterization.

II. Operation Scheme

The SOA response measurements were made on two 1-mm-long SOAs arranged in a five-port SOA-MZI (model 07.4059. LI1.WSP08 from Heinrich Hertz Institut), as shown at the top of Fig. 1.

A gain-switched distributed feedback (DFB) laser diode was used as the signal source to produce 1551-nm pulses at 10 GHz. A length of dispersion-compensating fiber was used following the DFB laser to compensate for the chirps of the generated pulses. A Mach–Zehnder modulator (MZM) driven with an alternating bit pattern was used to halve the repetition rate of the pulse train from 10 to 5 GHz. The lower repetition rate was chosen to allow the SOAs sufficient recovery time and thereby to avoid patterning effects. It was not a limitation of the measurement technique. The 5-GHz pulse train was then split into two arms, one of which became the pump signal into the SOA-MZI. At launch into the SOA-MZI, the pump pulses were 4.5 ps (full-width at half-maximum) and have a time-bandwidth product of 0.66.

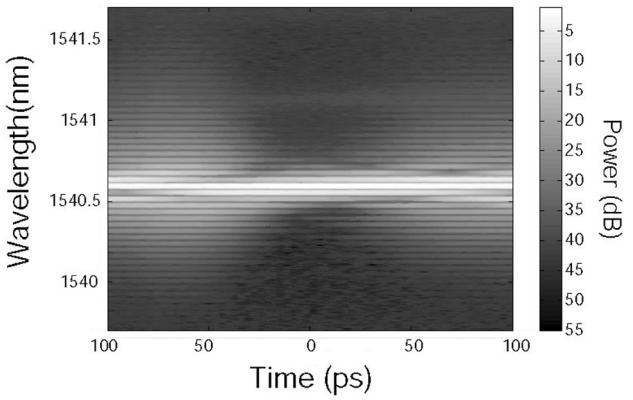

Fig. 2. Measured spectrogram for pump power= −10 dBm.

A second continuous-wave (CW) laser signal at 1540.6 nm acted as the probe to the SOA-MZI. L-FROG is implemented by constructing the cross-correlation of the probe signal with a second (electrical) signal on an optical spectrum analyzer (OSA). To achieve this, the pulse train in the second arm was converted to electrical pulses with a 20-GHz bandwidth photodetector and used to drive a $LiNbO_3$ MZM, where the cross-correlation (facilitated by temporal gating of the signal exiting from the SOA-MZI) took place. A variable optical delay in the gate arm of the L-FROG shifted the gating function and the signal to be measured with respect to each other to build up a spectrogram of the cross-correlation between the signal and the gate. Fig. 2 shows the measurements for an average input power of −10 dBm. The 5-GHz lines of our pulse train can be clearly seen stretching across the spectrogram as can the broadened spectrum on the leading and trailing edges. Note also that since the L-FROG is a spectrally resolved measurement, we can selectively measure only the signal pulse by choosing an appropriate wavelength range on the OSA. The measured spectrogram is then numerically processed to filter out the noise, extract the spectral envelope from the 5-GHz spectral lines, and resample to a 256×256 grid. The intensity and phase of both the signal and the gate pulses can then be effectively retrieved from the resampled spectrogram by performing a blind deconvolution. The deconvolution algorithm we used was a variation of the principle components generalized projection algorithm detailed in [6].

III. XPM and XGM Experiments

The SOA gain dynamics are determined by the variations of the total carrier density and its energy distribution within the conduction and valence bands. Depending on the width of the pulses we introduce in the SOA, the dominating effect in the gain dynamics change.

When the SOA is operated using pulses as short as a few picoseconds, intraband effects become important. Furthermore, using short pulses the output pulse saturation energy is pulsewidth-dependent [1]. The shorter the pump pulses, the larger the compression associated with the intraband effects [7]. Then, the gain compression associated with the intraband transitions has similar magnitude as compared to the compression associated with the interband transitions. In order to use the SOA intraband fast dynamics for high-speed applications, the slow gain compression should be kept as small as possible

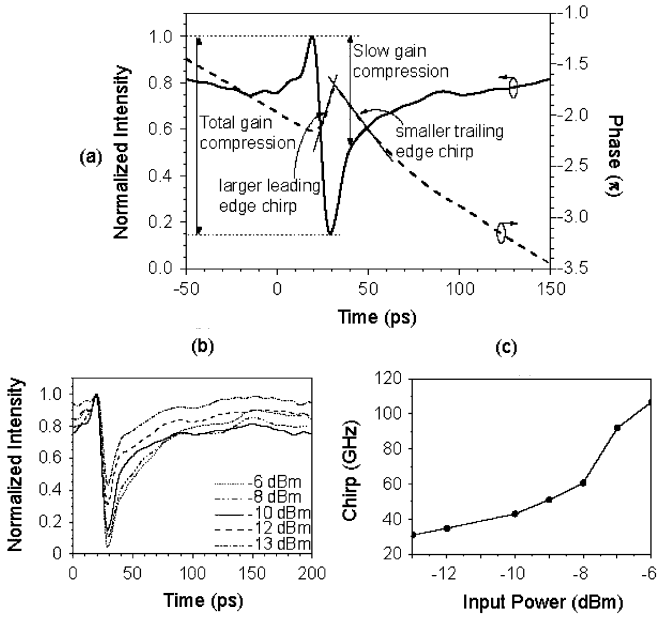

Fig. 3. (a) Measured intensity and phase for pump power = −10 dBm. (b) Measured probe transmission pulses for different pump powers. (c) Maximum (leading edge) chirp for XGM at different pump powers.

because of its slower dynamics. Using subpicosecond pulses it is possible to keep the slow gain compression small, even for input pulse energies higher than E_{satin}. This is not possible in the case of longer pulses, where the slow gain compression would be much larger because of the much higher contribution of the interband effects on the SOA saturation [9].

A. XGM

In this section, we describe measurements of XGM carved inverted and converted pulses using the L-FROG technique. For these measurements, we illuminated only SOA1 of the MZI-SOA (see Fig. 1). We measured the amplitude and phase of the probe using the L-FROG system. Fig. 3(a) shows the intensity and phase profile of the converted pulses when the pump pulses had an average power of −10 dBm. An inverted converted signal, typical of the XGM process, can clearly be observed. The phase profile shows that there is a large red shift (negative chirp) associated with the steep leading edge of the pulse and a smaller blue shift (positive chirp) associated with the shallow trailing edge of the pulse as a result of the slow response time. These phase changes arise from the nonlinear refractive index variations in the amplifier, and result in a chirp [1]. Similar intensity and phase profiles were obtained for different average pump input powers from −13 to −6 dBm (1.5-, 2.5-, 4-, 6-, 8-, and 10-mW peak powers). These intensity profiles can be seen in Fig. 3(b). The plots are normalized with respect to the maximum power of the probe signal at the output of the SOA. The total gain compression is the ratio of the unsaturated probe level to the minimum of the probe transmission. As expected, both total and slow gain compression increases with increasing pump energy which is in agreement with the theory. The increase in total gain compression is mainly due to the increase of the plasma temperature in the active region, which is caused by the increase in pump energy. The slow gain compression increases because of the reduced carrier density due to the increasing stimulated emission.

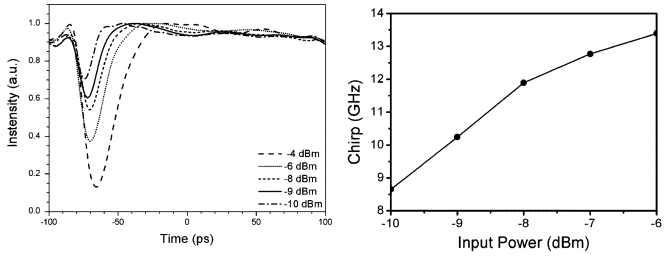

Fig. 4. (a) Measured SOA-MZI output pulses for different average pump powers. (b) Maximum (leading edge) chirp of the output pulses for different pump input powers.

After compression induced by the pump, the gain shows a fast recovery, resulting from intraband effects, mainly carrier heating and spectral hole burning. Faster effects, like two photon absorption would only play a main role for shorter pulses (femtosecond). After the fast gain recovery, the gain is recovering toward the unsaturated value as a result of electrical pumping. This interband recovery becomes shorter for longer SOA devices and for higher electrical bias currents [1]. Typical values for the 10%–90% recovery time are less than 50 ps for 2500 μm long, strongly biased SOAs, and up to 1 ns for shorter SOAs (250 μm). We see that the measurements we have obtained with the L-FROG system are in agreement with this statement. Since the repetition rate in our measurements was 200 ps, at low powers, the gain was able to fully recover to its unsaturated value in the 1-mm-long SOA devices that we experimented with.

Fig. 3(c) shows the peak chirp experienced by the pulse for increasing pump powers. We note that the peak chirp gradually increased from -30 to -105 GHz due to carrier-induced index changes. Since the recovery time due to intraband effects is affected by the input power, we have a variation of 75 GHz in the maximum observed chirp for 7-dB variation in power input. These and the previous results are in agreement with characterization measurements obtained using different techniques [1].

B. Mach–Zehnder Configuration

Having measured the response of a single SOA, in this section, we use the L-FROG to look at the effect of using the wavelength-converted pulses in a Mach–Zehnder interferometric configuration. The input pulses were generated in the same way as for the XGM case, but we now operate the SOA-MZI with both SOAs active. The XPM we observed in SOA1 can now interfere with the CW output from SOA2, and be converted to intensity modulation. Thus, at the output of the SOA-MZI, we obtain pulses which are primarily dependent on the XPM in SOA1, but also receive some shaping from the gain compression.

In this part of our experiment, SOAs 1 and 2 were operated at current values of $I1 = 300$ mA and $I2 = 160$ mA, respectively. These currents were selected for out-of-phase operation of the SOA-MZI to give inverted pulses. This mode of operation yields an opposite sign in the frequency chirp of the converted signal to that obtained when the device is operated in the in-phase operation mode.

Fig. 4 shows the L-FROG measured intensity profiles of the SOA-MZI output pulses. Average input peak powers between -10 and -4 dBm (3.8-, 4.5-, 6-, 8-, and 10-mW peak powers) were used to see the phase and amplitude dependence of the wavelength-converted output on input pump energy. We observe that as in the XGM case, both the total and slow gain compression increase with increasing pump energy. Likewise in Fig. 4(b), the chirp of the output pulses is shown to increase with increasing pump energy.

Further, comparing the amount of frequency chirp induced in the probe signal at the output of the SOA-MZI to that measured after XGM only, we note that the chirp at the output is much lower than that observed in XGM.

This difference here is due to the interference at the output and is consistent with the theory presented in [9]. Since the output of the MZI is given by the difference between the fields of the two arms, the maximum chirp excursion is reduced. As a result, using the Mach–Zehnder configuration produces pulses with lower chirp than when using XGM alone and so is more favorable for fiber transmission applications.

IV. Conclusion

We have performed XGM and XPM characterization measurements of 1-mm-long SOAs operated in a single SOA and in Mach–Zehnder configurations. We have fully characterized the dynamic response of the SOA-MZI to short picosecond pulses at 5 GHz using an L-FROG system employing a fast $LiNbO_3$ MZM as the sampling gate. Our measurements demonstrate the applicability of the L-FROG technique for the characterization of the dynamic response of fast optical devices, providing full phase and intensity profiling with good stability.

References

[1] L. Schares, C. Schubert, C. Schmidt, H. G. Weber, L. Occhi, and G. Guekos, "Phase dynamics of semiconductor optical amplifiers at 10–40 GHz," *IEEE J. Quantum Electron.*, vol. 39, no. 11, pp. 1394–1408, Nov. 2003.

[2] F. Gigarding, G. Guekos, and A. Houbavlis, "Gain recovery of bulk semiconductor optical amplifiers," *IEEE Photon. Technol. Lett.*, vol. 10, no. 6, pp. 784–786, Jun. 1998.

[3] C. Dorrer and I. Kang, "Simultaneous temporal characterisation of telecommunication pulses and modulators by use of spectrograms," *Opt. Lett.*, vol. 27, pp. 1315–1317, 2002.

[4] M. A. F. Roelens, P. Petropoulos, D. J. Richardson, M. Forzati, A. Djupsjobacka, and A. Bernston, "Linear frequency resolved optical gating as a line monitoring tool," in *Proc. OFC*, Anaheim, CA, 2006, Paper OWN2.

[5] C. Tian, Z. Zhang, M. A. F. Roelens, P. Petropoulos, M. Ibsen, and D. J. Richardson, "Full characterisation of the temporal response of phase-shifted SSFBGs using electroabsorption modulator based frequency resolved optical gating," in *Proc. BGPP/ACOFT*, Sydney, Australia, 2005.

[6] D. J. Kane, "Recent progress toward real-time measurement of ultrashort laser pulses," *IEEE J. Quantum Electron.*, vol. 35, no. 4, pp. 421–431, Apr. 1999.

[7] K. L. Hall, G. Lenz, A. M. Darwish, and E. P. Ippen, "Subpicosecond gain and index nonlinearities in InGaAsP diode lasers," *Opt. Commun.*, vol. 111, pp. 589–612, 1994.

[8] H. Lee, H. Yoon, Y. Kim, and J. Jeong, "Theoretical study of frequency chirping and extinction ratio of wavelength-converted optical signals by XGM and XPM using SOA's," *IEEE J. Quantum Electron.*, vol. 35, no. 8, pp. 1213–1219, Aug. 1999.

[9] L. Ochi, "Semiconductor Optical Amplifiers Made of Ridge Waveguide Bulk inGaAsP/InP," Ph.D. Thesis, ETH-Zurich, Zurich, Switzerland, 2002.